Measurement of the Midrapidity Transverse Energy Distribution from $\sqrt{s_{NN}} = 130$ GeV Au + Au Collisions at RHIC

K. Adcox,[40] S. S. Adler,[3] N. N. Ajitanand,[27] Y. Akiba,[14] J. Alexander,[27] L. Aphecetche,[34] Y. Arai,[14] S. H. Aronson,[3] R. Averbeck,[28] T. C. Awes,[29] K. N. Barish,[5] P. D. Barnes,[19] J. Barrette,[21] B. Bassalleck,[25] S. Bathe,[22] V. Baublis,[30] A. Bazilevsky,[12,32] S. Belikov,[12,13] F. G. Bellaiche,[29] S. T. Belyaev,[16] M. J. Bennett,[19] Y. Berdnikov,[35] S. Botelho,[33] M. L. Brooks,[19] D. S. Brown,[26] N. Bruner,[25] D. Bucher,[22] H. Buesching,[22] V. Bumazhnov,[12] G. Bunce,[3,32] J. Burward-Hoy,[28] S. Butsyk,[28,30] T. A. Carey,[19] P. Chand,[2] J. Chang,[5] W. C. Chang,[1] L. L. Chavez,[25] S. Chernichenko,[12] C. Y. Chi,[8] J. Chiba,[14] M. Chiu,[8] R. K. Choudhury,[2] T. Christ,[28] T. Chujo,[3,39] M. S. Chung,[15,19] P. Chung,[27] V. Cianciolo,[29] B. A. Cole,[8] D. G. D'Enterria,[34] G. David,[3] H. Delagrange,[34] A. Denisov,[12] A. Deshpande,[32] E. J. Desmond,[3] O. Dietzsch,[33] B. V. Dinesh,[2] A. Drees,[28] A. Durum,[12] D. Dutta,[2] K. Ebisu,[24] Y. V. Efremenko,[29] K. El Chenawi,[40] H. En'yo,[17,31] S. Esumi,[39] L. Ewell,[3] T. Ferdousi,[5] D. E. Fields,[25] S. L. Fokin,[16] Z. Fraenkel,[42] A. Franz,[3] A. D. Frawley,[9] S.-Y. Fung,[5] S. Garpman,[20] T. K. Ghosh,[40] A. Glenn,[36] A. L. Godoi,[33] Y. Goto,[32] S. V. Greene,[40] M. Grosse Perdekamp,[32] S. K. Gupta,[2] W. Guryn,[3] H.-Å. Gustafsson,[20] J. S. Haggerty,[3] H. Hamagaki,[7] A. G. Hansen,[19] H. Hara,[24] E. P. Hartouni,[18] R. Hayano,[38] N. Hayashi,[31] X. He,[10] T. K. Hemmick,[28] J. M. Heuser,[28] M. Hibino,[41] J. C. Hill,[13] D. S. Ho,[43] K. Homma,[11] B. Hong,[15] A. Hoover,[26] T. Ichihara,[31,32] K. Imai,[17,31] M. S. Ippolitov,[16] M. Ishihara,[31,32] B. V. Jacak,[28,32] W. Y. Jang,[15] J. Jia,[28] B. M. Johnson,[3] S. C. Johnson,[18,28] K. S. Joo,[23] S. Kametani,[41] J. H. Kang,[43] M. Kann,[30] S. S. Kapoor,[2] S. Kelly,[8] B. Khachaturov,[42] A. Khanzadeev,[30] J. Kikuchi,[41] D. J. Kim,[43] H. J. Kim,[43] S. Y. Kim,[43] Y. G. Kim,[43] W. W. Kinnison,[19] E. Kistenev,[3] A. Kiyomichi,[39] C. Klein-Boesing,[22] S. Klinksiek,[25] L. Kochenda,[30] D. Kochetkov,[5] V. Kochetkov,[12] D. Koehler,[25] T. Kohama,[11] A. Kozlov,[42] P. J. Kroon,[3] K. Kurita,[31,32] M. J. Kweon,[15] Y. Kwon,[43] G. S. Kyle,[26] R. Lacey,[27] J. G. Lajoie,[13] J. Lauret,[27] A. Lebedev,[13] D. M. Lee,[19] M. J. Leitch,[19] X. H. Li,[5] Z. Li,[6,31] D. J. Lim,[43] M. X. Liu,[19] X. Liu,[6] Z. Liu,[6] C. F. Maguire,[40] J. Mahon,[3] Y. I. Makdisi,[3] V. I. Manko,[16] Y. Mao,[6,31] S. K. Mark,[21] S. Markacs,[8] G. Martinez,[34] M. D. Marx,[28] A. Masaike,[17] F. Matathias,[28] T. Matsumoto,[7,41] P. L. McGaughey,[19] E. Melnikov,[12] M. Merschmeyer,[22] F. Messer,[28] M. Messer,[3] Y. Miake,[39] T. E. Miller,[40] A. Milov,[42] S. Mioduszewski,[3,36] R. E. Mischke,[19] G. C. Mishra,[10] J. T. Mitchell,[3] A. K. Mohanty,[2] D. P. Morrison,[3] J. M. Moss,[19] F. Mühlbacher,[28] M. Muniruzzaman,[5] J. Murata,[31] S. Nagamiya,[14] Y. Nagasaka,[24] J. L. Nagle,[8] Y. Nakada,[17] B. K. Nandi,[5] J. Newby,[36] L. Nikkinen,[21] P. Nilsson,[20] S. Nishimura,[7] A. S. Nyanin,[16] J. Nystrand,[20] E. O'Brien,[3] C. A. Ogilvie,[13] H. Ohnishi,[3,11] I. D. Ojha,[4,40] M. Ono,[39] V. Onuchin,[12] A. Oskarsson,[20] L. Österman,[20] I. Otterlund,[20] K. Oyama,[7,38] L. Paffrath,[3,*] A. P. T. Palounek,[19] V. S. Pantuev,[28] V. Papavassiliou,[26] S. F. Pate,[26] T. Peitzmann,[22] A. N. Petridis,[13] C. Pinkenburg,[3,27] R. P. Pisani,[3] P. Pitukhin,[12] F. Plasil,[29] M. Pollack,[28,36] K. Pope,[36] M. L. Purschke,[3] I. Ravinovich,[42] K. F. Read,[29,36] K. Reygers,[22] V. Riabov,[30,35] Y. Riabov,[30] M. Rosati,[13] A. A. Rose,[40] S. S. Ryu,[43] N. Saito,[31,32] A. Sakaguchi,[11] T. Sakaguchi,[7,41] H. Sako,[39] T. Sakuma,[31,37] V. Samsonov,[30] T. C. Sangster,[18] R. Santo,[22] H. D. Sato,[17,31] S. Sato,[39] S. Sawada,[14] B. R. Schlei,[19] Y. Schutz,[34] V. Semenov,[12] R. Seto,[5] T. K. Shea,[3] I. Shein,[12] T.-A. Shibata,[31,37] K. Shigaki,[14] T. Shiina,[19] Y. H. Shin,[43] I. G. Sibiriak,[16] D. Silvermyr,[20] K. S. Sim,[15] J. Simon-Gillo,[19] C. P. Singh,[4] V. Singh,[4] M. Sivertz,[3] A. Soldatov,[12] R. A. Soltz,[18] S. Sorensen,[29,36] P. W. Stankus,[29] N. Starinsky,[21] P. Steinberg,[8] E. Stenlund,[20] A. Ster,[44] S. P. Stoll,[3] M. Sugioka,[31,37] T. Sugitate,[11] J. P. Sullivan,[19] Y. Sumi,[11] Z. Sun,[6] M. Suzuki,[39] E. M. Takagui,[33] A. Taketani,[31] M. Tamai,[41] K. H. Tanaka,[14] Y. Tanaka,[24] E. Taniguchi,[31,37] M. J. Tannenbaum,[3] J. Thomas,[28] J. H. Thomas,[18] T. L. Thomas,[25] W. Tian,[6,36] J. Tojo,[17,31] H. Torii,[17,31] R. S. Towell,[19] I. Tserruya,[42] H. Tsuruoka,[39] A. A. Tsvetkov,[16] S. K. Tuli,[4] H. Tydesjö,[20] N. Tyurin,[12] T. Ushiroda,[24] H. W. van Hecke,[19] C. Velissaris,[26] J. Velkovska,[28] M. Velkovsky,[28] A. A. Vinogradov,[16] M. A. Volkov,[16] A. Vorobyov,[30] E. Vznuzdaev,[30] H. Wang,[5] Y. Watanabe,[31,32] S. N. White,[3] C. Witzig,[3] F. K. Wohn,[13] C. L. Woody,[3] W. Xie,[5,42] K. Yagi,[39] S. Yokkaichi,[31] G. R. Young,[29] I. E. Yushmanov,[16] W. A. Zajc,[8] Z. Zhang,[28] and S. Zhou[6]

(PHENIX Collaboration)

[1]*Institute of Physics, Academia Sinica, Taipei 11529, Taiwan*
[2]*Bhabha Atomic Research Centre, Bombay 400 085, India*
[3]*Brookhaven National Laboratory, Upton, New York 11973-5000*
[4]*Department of Physics, Banaras Hindu University, Varanasi 221005, India*
[5]*University of California–Riverside, Riverside, California 92521*
[6]*China Institute of Atomic Energy (CIAE), Beijing, People's Republic of China*
[7]*Center for Nuclear Study, Graduate School of Science, University of Tokyo, 7-3-1 Hongo, Bunkyo, Tokyo 113-0033, Japan*

 0031-9007/01/87(5)/052301(6)$15.00

[8]*Columbia University, New York, New York 10027 and Nevis Laboratories, Irvington, New York 10533*
[9]*Florida State University, Tallahassee, Florida 32306*
[10]*Georgia State University, Atlanta, Georgia 30303*
[11]*Hiroshima University, Kagamiyama, Higashi-Hiroshima 739-8526, Japan*
[12]*Institute for High Energy Physics (IHEP), Protvino, Russia*
[13]*Iowa State University, Ames, Iowa 50011*
[14]*KEK, High Energy Accelerator Research Organization, Tsukuba-shi, Ibaraki-ken 305-0801, Japan*
[15]*Korea University, Seoul, 136-701, Korea*
[16]*Russian Research Center, "Kurchatov Institute," Moscow, Russia*
[17]*Kyoto University, Kyoto 606, Japan*
[18]*Lawrence Livermore National Laboratory, Livermore, California 94550*
[19]*Los Alamos National Laboratory, Los Alamos, New Mexico 87545*
[20]*Department of Physics, Lund University, Box 118, SE-221 00 Lund, Sweden*
[21]*McGill University, Montreal, Quebec, Canada H3A 2T8*
[22]*Institut für Kernphysik, University of Münster, D-48149 Münster, Germany*
[23]*Myongji University, Yongin, Kyonggido 449-728, Korea*
[24]*Nagasaki Institute of Applied Science, Nagasaki-shi, Nagasaki 851-0193, Japan*
[25]*University of New Mexico, Albuquerque, New Mexico 87131*
[26]*New Mexico State University, Las Cruces, New Mexico 88003*
[27]*Chemistry Department, State University of New York–Stony Brook, Stony Brook, New York 11794*
[28]*Department of Physics and Astronomy, State University of New York–Stony Brook, Stony Brook, New York 11794*
[29]*Oak Ridge National Laboratory, Oak Ridge, Tennessee 37831*
[30]*PNPI, Petersburg Nuclear Physics Institute, Gatchina, Russia*
[31]*RIKEN (The Institute of Physical and Chemical Research), Wako, Saitama 351-0198, Japan*
[32]*RIKEN BNL Research Center, Brookhaven National Laboratory, Upton, New York 11973-5000*
[33]*Universidade de São Paulo, Instituto de Física, Caixa Postal 66318, São Paulo CEP05315-970, Brazil*
[34]*SUBATECH (Ecole des Mines de Nantes, IN2P3/CNRS, Universite de Nantes) BP 20722-44307, Nantes-Cedex 3, France*
[35]*St. Petersburg State Technical University, St. Petersburg, Russia*
[36]*University of Tennessee, Knoxville, Tennessee 37996*
[37]*Department of Physics, Tokyo Institute of Technology, Tokyo, 152-8551, Japan*
[38]*University of Tokyo, Tokyo, Japan*
[39]*Institute of Physics, University of Tsukuba, Tsukuba, Ibaraki 305, Japan*
[40]*Vanderbilt University, Nashville, Tennessee 37235*
[41]*Waseda University, Advanced Research Institute for Science and Engineering, 17 Kikui-cho, Shinjuku-ku, Tokyo 162-0044, Japan*
[42]*Weizmann Institute, Rehovot 76100, Israel*
[43]*Yonsei University, IPAP, Seoul 120-749, Korea*
[44]*KFKI Research Institute for Particle and Nuclear Physics (RMKI), Budapest, Hungary*[†]

(Received 18 April 2001; published 17 July 2001)

The first measurement of energy produced transverse to the beam direction at the Relativistic Heavy-Ion Collider at Brookhaven National Laboratory is presented. The midrapidity transverse energy density per participating nucleon rises steadily with the number of participants, closely paralleling the rise in charged-particle density, such that $\langle E_T\rangle/\langle N_{ch}\rangle$ remains relatively constant as a function of centrality. The energy density calculated via Bjorken's prescription for the 2% most central Au + Au collisions at $\sqrt{s_{NN}} = 130$ GeV is at least $\epsilon_{Bj} = 4.6\ \mathrm{GeV/fm^3}$, which is a factor of 1.6 larger than found at $\sqrt{s_{NN}} = 17.2$ GeV (Pb + Pb at CERN).

DOI: 10.1103/PhysRevLett.87.052301 PACS numbers: 25.75.–q, 12.38.Mh, 13.60.Le, 13.85.Hd

The PHENIX detector [1] at RHIC, the Relativistic Heavy-Ion Collider at Brookhaven National Laboratory, is designed to measure the properties of nuclear matter at the highest temperatures and energy densities. For example, a transition to a quark-gluon plasma has been predicted for energy densities on the order of a few $\mathrm{GeV/fm^3}$ [2]. The spatial energy density (ϵ) in a relativistic collision can be estimated (following Bjorken [3]) by measuring the transverse energy density in rapidity, dE_T/dy, which is effectively the comoving energy density in a longitudinal expansion:

$$\epsilon_{Bj} = \frac{dE_T}{dy}\,\frac{1}{\tau_0 \pi R^2}\,, \tag{1}$$

where τ_0, the formation time, is usually taken as 1 fm/c, and πR^2 is the effective area of the collision. The transverse energy (E_T) is a multiparticle variable defined as

$$\begin{aligned} E_T &= \sum_i E_i \sin\theta_i\,, \\ dE_T(\eta)/d\eta &= \sin\theta(\eta)\, dE(\eta)/d\eta\,, \end{aligned} \tag{2}$$

where θ is the polar angle, $\eta = -\ln\tan\theta/2$ is the pseudorapidity, E_i is by convention taken as the kinetic energy for nucleons and the total energy for all other particles [4], and the sum is taken over all particles emitted into a fixed solid angle for each event. E_T measurements, even in limited apertures at midrapidity, provide excellent characterization of the nuclear geometry of a reaction on an event-by-event basis and are sensitive to the underlying reaction dynamics [2].

During the RHIC run in the summer of 2000, PHENIX accumulated close to 5×10^6 interaction triggers for Au + Au collisions at $\sqrt{s_{NN}} = 130$ GeV using zero degree calorimeters and beam-beam counters (BBC) as triggering devices. The events were selected with a requirement on the collision vertex position along the beam axis, $|z| \leq 20$ cm, as in the recent PHENIX publication on midrapidity multiplicity distributions [5], where further details are given.

The present measurement uses a section of the electromagnetic calorimeter (EMCal) from the PHENIX central spectrometer, with front face 5.1 m from the beam axis. This section is part of a sampling calorimeter, custom developed and built for PHENIX [6], composed of alternating Pb and scintillator tiles (PbSc) with readout of individual towers, 5.54×5.54 cm^2 in cross section, via wavelength shifting fibers in a "shashlik" geometry. The depth of the PbSc calorimeter is 18 radiation lengths (X_0) which corresponds to 0.85 interaction lengths. The PbSc calorimeter has an energy resolution of $8.2\%/\sqrt{E(\mathrm{GeV})} \oplus 1.9\%$ for test beam electrons, with measured response proportional to incident electron energy to within $\pm 2\%$ over the range $0.3 \leq E_e \leq 40.0$ GeV [6].

During construction, the calibration of the calorimeter was set by simultaneously recording the response to laser excitation and to cosmic-ray muons penetrating transversely to the tower axis. The calibration was maintained *in situ* during the run by monitoring relativistic charged particles from Au + Au collisions. The absolute energy scale was determined by test-beam measurements normalized to electrons with known energy. A final adjustment of the absolute energy scale was performed using *in situ* identified electrons ($p > 500$ MeV/c) by shifting the originally measured energy/momentum (E/p) peak from 1.02 ± 0.01 to 1.00. The accuracy of the absolute energy scale was cross-checked *in situ* against both the minimum ionizing peak (MIP) of charged particles penetrating along the tower axis and the mass of the π^0. The corrected energy distribution of EMCal clusters from 1.0 ± 0.1 GeV/c charged tracks (mostly pions) measured in the drift chamber [1] exhibits a clear MIP (Fig. 1a), as well as energy due to nuclear interactions in the material of the EMCal. The MIP position is in agreement within 2% to the value obtained in the test beam (270 MeV). The mass of the π^0, reconstructed from pairs of EMCal clusters (assumed to be photons [7]) of total energy greater than 2 GeV (Fig. 1b), is within 1.5% of the published value. This sets the systematic error of the absolute energy scale at less than 1.5%.

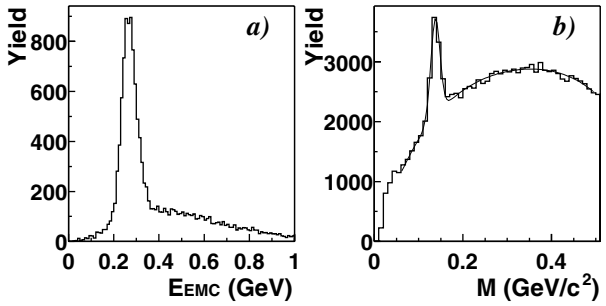

FIG. 1. (a) The distribution of EMCal clusters corresponding to 1 GeV/c charged tracks (mostly pions) from Au + Au collisions. (b) The reconstructed π^0 mass from pairs of EMCal clusters with total energy >2 GeV.

The data sample for the present E_T measurement is taken from the same runs used in our multiplicity measurement [5] (no magnetic field) and comprises about 140 000 events from the BBC trigger which detects $[92 \pm 2(\mathrm{syst})]\%$ of the nuclear interaction cross section of 7.2 b with a background contamination of $[1 \pm 1(\mathrm{syst})]\%$ [5]. The transverse energy was measured using the PbSc EMCal in a fiducial aperture $|\eta| \leq 0.38$ in pseudorapidity and $\Delta\phi = 44.4°$ in azimuth. E_T was computed for each event [Eq. (2)] using clusters of energy greater than 20 MeV, composed of adjacent towers with deposited energy of more than 3 MeV. The angle θ_i is computed from the centroid of the cluster of energy E_i assuming a particle originating from the event vertex.

The raw spectrum of measured transverse energy, $E_{T\mathrm{EMC}}$, in the fiducial aperture of the PHENIX EMCal for Au + Au collisions at $\sqrt{s_{NN}} = 130$ GeV is shown in Fig. 2, upper scale. The lower scale in Fig. 2 represents a correction of the raw $E_{T\mathrm{EMC}}$ by a factor of 12.8 to correspond to the hadronic $dE_T/d\eta|_{\eta=0}$ in the full azimuth. The 12.8 is composed of a factor of 10.6 for the fiducial acceptance, a factor of 1.03 for disabled calorimeter towers and a factor, $k = 1.17 \pm 0.01$, which is the ratio of the hadronic E_T in the fiducial aperture to the measured $E_{T\mathrm{EMC}}$. The k factor includes the response of the detector to charged and neutral particles emitted from the event vertex into the fiducial aperture, and additional corrections for energy inflow from outside the fiducial aperture and for losses [8]. These factors were calculated with a GEANT [9] based Monte Carlo (MC) simulation of the detector using HIJING as the event generator [10].

For E_T measurements at midrapidity at a collider, the EMCal acts as a thin but effective hadronic calorimeter. Charged pions with $p_T \leq 0.35$ GeV/c, kaons ($p_T \leq 0.64$ GeV/c), and protons ($p_T \leq 0.94$ GeV/c)—p_T values which are near or above the $\langle p_T \rangle$ for all three cases—stop (i.e., deposit all their kinetic energy) in the EMCal. For higher p_T hadrons, 43% leave the MIP and 57% interact, leaving an average of ~65% of their energy.

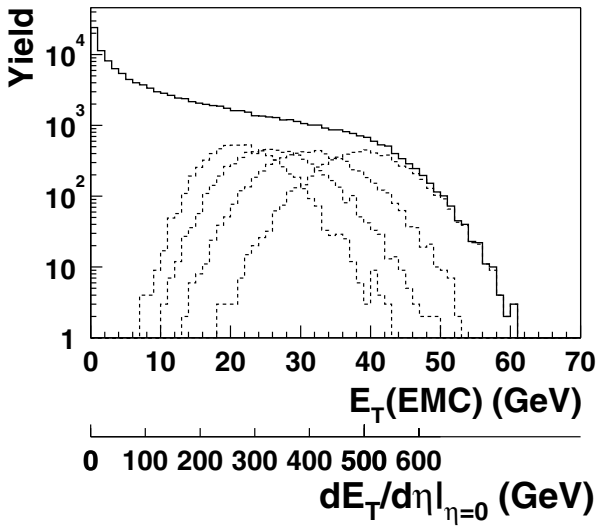

FIG. 2. The raw $E_{T\mathrm{EMC}}$ distribution measured in the $\Delta\phi = 44.4°$ azimuthal and $|\eta| \leq 0.38$ polar angle fiducial acceptance for Au + Au at $\sqrt{s_{NN}} = 130$ GeV (upper scale) and total hadronic $dE_T/d\eta|_{\eta=0}$ (lower scale); see text. The solid line is the minimum bias distribution with the BBC trigger; the dashed lines correspond to the distributions for the four most central bins in Table I.

The measured $E_{T\mathrm{EMC}}$ is 0.79 ± 0.01 of the total E_T striking the EMCal, which is composed roughly of 40% produced by charged pions, 40% by photons (from π^0 and other decays), and 20% by all other particles (including decay muons). The particle composition and $\langle p_T \rangle$ in HIJING are close to the observed values, and furthermore, the k factor is insensitive to reasonable variations (for instance, varying the momenta of all particles by $\pm 15\%$ changes the overall k by less than $\pm 2\%$), leading to an estimated systematic uncertainty in k of less than $\pm 3\%$ due to particle composition and momentum.

The main issues for the MC are the inflow contribution and losses. The losses are due to particles which originate within the aperture but whose decay products miss the EMCal (10%), or whose energy is lost due to edge effects (6%) or clustering (2%). The inflow, $(24 \pm 1)\%$ of the E_T striking the EMCal, is principally of two types: (i) albedo from the magnet poles and (ii) particles which originate outside the aperture of the calorimeter but whose decay products hit the calorimeter. The inflow component of k was checked by comparing the MC and the measurements for events with a vertex outside the normal range, just at and inside a pole face of the axial central-spectrometer magnet, $38 \leq z \leq 42$ cm, for which the calorimeter aperture is partly shadowed. The fraction of the total energy, $dE_{\mathrm{EMC}}/E_{\mathrm{EMC}}$, in bins of width 2 towers along the z coordinate of the EMCal, z_{EMC}, is shown in Fig. 3a. The HIJING MC simulation agrees with the measured data everywhere except in the range $z_{\mathrm{EMC}} > 100$ cm, which is fully shadowed by the pole, where the simulation shows $\sim 20\%$ less energy than the data. In Fig. 3b, the distributions of the cluster energy, E_{cl}, for the open aperture, $z_{\mathrm{EMC}} < -50$ cm, are shown for both HIJING and the data and are in excellent agreement. The inflow component of HIJING is also indicated as a dotted line and falls much more sharply than the total E_{cl} spectrum. The residual discrepancy of the energy in the shadowed region, which contributes roughly 10% of the total signal, results in a $\pm(2 - 3)\%$ systematic uncertainty in E_T due to the uncertainty in the inflow. Combining this with the uncertainty due to particle composition and momentum yields an overall factor $k = [1.17 \pm 0.01] \pm 4\%$ (syst), which, according to the MC, is independent of centrality.

Returning to Fig. 2, the shape of the measured transverse energy spectrum shows the characteristic form of E_T distributions in limited apertures: a peak and a sharp dropoff at low values of E_T corresponding to peripheral collisions with grazing impact; a broad, gently sloping plateau at the midrange of impact parameters, dominated by the nuclear geometry; and then at higher values of E_T, which correspond to the most central collisions where the nuclei are fully overlapped, a "knee" leading to a falloff which is very steep for large apertures and which becomes less steep, the smaller the aperture [11]. It should be emphasized that the correction of $E_{T\mathrm{EMC}}$ to $dE_T/d\eta|_{\eta=0}$

TABLE I. Average transverse energy density vs centrality. The statistical errors are negligible. Errors on $\langle dE_T/d\eta|_{\eta=0} \rangle$ are the N_{part}-dependent systematic errors from the uncertainty of the BBC cross section [5] such that all points move together. There is an additional overall (N_{part}-independent) systematic uncertainty of $\pm 4.5\%$.

Centrality	$\langle dE_T/d\eta|_{\eta=0} \rangle$ (GeV)	$\langle dN_{ch}/d\eta|_{\eta=0} \rangle$ [5]	$\langle N_{\mathrm{part}} \rangle$ [5]
0%–5%	503 ± 2	622 ± 41	347 ± 10
5%–10%	409 ± 4	498 ± 31	293 ± 9
10%–15%	340 ± 5	413 ± 25	248 ± 8
15%–20%	283 ± 7	344 ± 21	211 ± 7
20%–25%	233 ± 7	287 ± 18	177 ± 7
25%–30%	191 ± 8	235 ± 16	146 ± 6
30%–35%	154 ± 8	188 ± 14	122 ± 5
35%–40%	123 ± 7	147 ± 12	99 ± 5
40%–45%	98 ± 7	115 ± 11	82 ± 5
45%–50%	76 ± 6	89 ± 9	68 ± 4

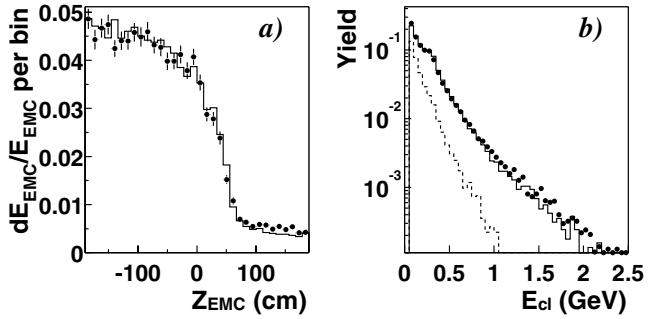

FIG. 3. (a) The fraction of $E_{T\mathrm{EMC}}$ in bins of 11.08 cm along the EMCal z_{EMC} direction for event vertex near a pole face; histogram from MC simulation and solid points from beam data. (b) EMCal cluster energy spectrum from HIJING MC (solid line), with inflow component (dotted line) compared to data (solid points).

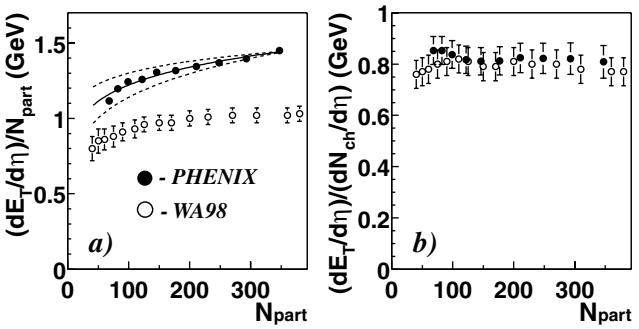

FIG. 4. (a) PHENIX transverse energy density per participant $dE_T/d\eta|_{\eta=0}/N_{\mathrm{part}}$ for Au + Au collisions at $\sqrt{s_{NN}} =$ 130 GeV as a function of N_{part}, the number of participants, compared to data from WA98 [12] for Pb + Pb collisions at $\sqrt{s_{NN}} = 17.2$ GeV. The solid line is the $N_{\mathrm{part}}^{\alpha}$ best fit and the dashed lines represent the effect of the $\pm 1\sigma$ N_{part}-dependent systematic errors for $dE_T/d\eta|_{\eta=0}$ and N_{part}. There is an additional overall (N_{part}-independent) systematic uncertainty of $\pm 4.5\%$ from $dE_T/d\eta|_{\eta=0}$ and $\pm 2.0\%$ from N_{part}. (b) PHENIX $dE_T/d\eta|_{\eta=0}/dN_{ch}/d\eta|_{\eta=0}$ versus N_{part}, including all systematic errors, compared to WA98. Note that the WA98 data in both (a) and (b) have an additional $\pm 20\%$ overall systematic error which is not shown.

by a single scale factor (predominantly acceptance) is valid up to the knee of the distribution, roughly the upper 1 percentile. Above the knee, the falloff depends on the aperture and is sensitive to detector effects as well as statistical and dynamical fluctuations. Thus an actual measurement of $dE_T/d\eta|_{\eta=0}$ for $\Delta\eta = 1.0$ and full azimuth would have a sharper falloff above the knee. With this caveat, the uncertainty in the absolute energy scale ($\pm 1.5\%$) and the uncertainty in k of $\pm 4\%$ are combined to yield an overall uncertainty in the hadronic $dE_T/d\eta|_{\eta=0}$ of $\pm 4.5\%$ (syst), independent of E_T, where the statistical error is negligible.

Midrapidity E_T distributions are a standard method of defining centrality [2,11–13]. Thus, it is important to determine for the present data the detailed relationship of transverse energy production to N_{part}, the number of nucleons participating in the collision (participants), which in earlier fixed target experiments was deduced straightforwardly by measuring the energy of spectator nucleons and fragments in a zero degree calorimeter at beam rapidity. Following a procedure used in our previous publication on the midrapidity charged multiplicity (N_{ch}) distribution, in which a clear increase of $\langle dN_{ch}/d\eta|_{\eta=0}\rangle$ per participant with the number of participants was demonstrated [5], we calculate $\langle dE_T/d\eta|_{\eta=0}\rangle$ as a function of centrality in upper percentile ranges of the 7.2 b Au + Au interaction cross section (see Table I). Figure 4a shows that $\langle dE_T/d\eta|_{\eta=0}\rangle$ per participant also increases with N_{part}, closely paralleling the rise in charged particle density (Table I). This is better illustrated in Fig. 4b where the ratio $\langle dE_T/d\eta|_{\eta=0}\rangle/\langle dN_{ch}/d\eta|_{\eta=0}\rangle$ remains constant at a value of ~ 0.8 GeV, independent of centrality. Comparison to the measurements of WA98 [12] from Pb + Pb collisions at $\sqrt{s_{NN}} = 17.2$ GeV is instructive. The WA98 data for midrapidity $\langle dE_T/d\eta|_{\mathrm{mid}}\rangle$ per participant are shown in Fig. 4a and are essentially independent of N_{part} for $N_{\mathrm{part}} > 200$ [14]. WA98 parametrizes their data as $dE_T/d\eta|_{\mathrm{mid}} \propto N_{\mathrm{part}}^{\alpha}$ with $\alpha = 1.08 \pm 0.06$ while the same parametrization for our data yields $\alpha = 1.13 \pm 0.05$. Figure 4 also shows that $\langle dE_T/d\eta|_{\eta=0}\rangle$ for central Au + Au collisions at $\sqrt{s_{NN}} = 130$ GeV is about 40% larger than found by WA98, yet, for both c.m. energies, $\langle dE_T/d\eta\rangle/\langle dN_{ch}/d\eta\rangle$ remains constant versus centrality at roughly the same value, ~ 0.8 GeV (Fig. 4b).

The Bjorken energy density for Pb + Pb collisions at $\sqrt{s_{NN}} = 17.2$ GeV was given by the NA49 Collaboration [13]. NA49 reported a value of midrapidity $dE_T/d\eta|_{\mathrm{mid}} = 405$ GeV for the most central 2% of the inelastic cross section, in agreement with WA98. This corresponds [13] to a value of $\epsilon_{Bj} = 2.9\ \mathrm{GeV/fm^3}$. A straightforward derivation of ϵ_{Bj} from our measured $dE_T/d\eta|_{\eta=0}$ of 578^{+26}_{-39} GeV for the same centrality cut, corrected to $dE_T/dy|_{y=0}$ by a factor of 1.19 ± 0.01 from our HIJING MC, and taking $\pi R^2 = 148\ \mathrm{fm^2}$ (i.e., $R = 1.18\ \mathrm{fm}\, A^{1/3}$) gives $\epsilon_{Bj} = 4.6\ \mathrm{GeV/fm^3}$, an increase of 60% over the NA49 value.

In conclusion, the midrapidity transverse energy density for central Au + Au collisions, and likely the spatial energy density, is at least 1.6 times larger at $\sqrt{s_{NN}} =$ 130 GeV (RHIC) than at $\sqrt{s_{NN}} = 17.2$ GeV (CERN). The variation of the E_T density per participant with centrality is very similar to the previously reported dependence of charged multiplicity density per participant at RHIC energies. These results, together with the observed constancy of $\langle E_T\rangle/\langle N_{ch}\rangle$ at a value ~ 0.8 GeV, indicate that the additional energy density at RHIC energies is achieved mainly by an increase in particle production rather than by an increase in transverse energy per particle.

We thank the staff of the RHIC project, Collider-Accelerator, and Physics Departments at BNL and the staff of PHENIX participating institutions for their vital

contributions. We acknowledge support from the Department of Energy and NSF (U.S.A.), Monbu-sho and STA (Japan), RAS, RMAE, and RMS (Russia), BMBF, DAAD, and AvH (Germany), FRN, NFR, and the Wallenberg Foundation (Sweden), MIST and NSERC (Canada), CNPq and FAPESP (Brazil), IN2P3/CNRS (France), DAE (India), KRF and KOSEF (Korea), and the U.S.–Israel Binational Science Foundation.

*Deceased.

†Not a participating institution (author is an individual participant).

[1] PHENIX Collaboration, D. P. Morrison *et al.,* Nucl. Phys. **A638**, 565c (1998).

[2] For example, see *Proceedings Quark Matter 1984,* edited by K. Kajantie (Springer, Berlin, 1985); *Proceedings Quark Matter 1987,* edited by H. Satz, H. J. Specht, and R. Stock [Z. Phys. C **38**, 1–370 (1988)].

[3] J. D. Bjorken, Phys. Rev. D **27**, 140 (1983).

[4] Helios Collaboration, T. Åkesson *et al.,* Z. Phys. C **38**, 383 (1988); **38**, 397 (1988).

[5] PHENIX Collaboration, K. Adcox *et al.,* Phys. Rev. Lett. **86**, 3500 (2001).

[6] E. Kistenev *et al.,* in *Proceedings of the 5th International Conference on Calorimetry in HEP* (World Scientific, Singapore, 1994), pp. 211–223; G. David *et al.,* IEEE Trans. Nucl. Sci. **45**, 692 (1998); **45**, 705 (1998).

[7] The PbSc EMCal measures ~GeV photons 2.1% higher than electrons of the same energy. This effect is corrected in Fig. 1b.

[8] $k = 1.17 = (1 - 0.24[\text{inflow}])/(0.79[\text{response}] \times \{1 - 0.18[\text{losses}]\})$

[9] GEANT 3.2.1, CERN program library.

[10] X. N. Wang and M. Gyulassy, Phys. Rev. D **44**, 3501 (1991), version 1.35.

[11] E802 Collaboration, T. Abbott *et al.,* Phys. Rev. C **63**, 064602 (2001).

[12] WA98 Collaboration, M. M. Aggarwal *et al.,* Eur. Phys. J. C **18**, 651 (2001).

[13] NA49 Collaboration, T. Alber *et al.,* Phys. Rev. Lett. **75**, 3814 (1995). (The quoted $\epsilon_{Bj} = 3.2$ GeV/fm^3 was divided by 1.10 to remove the enhancement factor applied by those authors for "head-on" collisions.)

[14] E_T is not Lorentz invariant; frame-dependent 10%–20% effects in comparing fixed target experiments to colliders are ignored in the present discussion.